Electronic Supplementary Information (ESI)

Color-Tunable Fluorescent Pillararene Coordination Polymer for Efficient Pollutant Detection

Xiang-Shuai Li,[ab] Yong-Fu Li,[a] Jia-Rui Wu,[a] Xin-Yue Lou,[a] Junyou Han,*[b] Jianchun Qin,*[b]

and Ying-Wei Yang*[ac]

[a]State Key Laboratory of Inorganic Synthesis and Preparative Chemistry, International Joint Research Laboratory of Nano-Micro Architecture Chemistry, College of Chemistry, Jilin University, 2699 Qianjin Street, Changchun 130012, P. R. China

[b]College of Plant Science, Jilin University, 5333 Xi'an Street, Changchun 130062, P. R. China

[c]The State Key Laboratory of Refractories and Metallurgy, School of Chemistry and Chemical Engineering, Wuhan University of Science and Technology, Wuhan 430081, P. R. China

*Corresponding authors: hanjy@jlu.edu.cn (J.H.); qinjc@jlu.edu.cn (J.Q.); ywyang@jlu.edu.cn (Y.-W.Y.)

1. Chemicals and Instruments

Terbium (III) chloride hexahydrate ($TbCl_3 \cdot 6H_2O$) and europium (III) chloride hexahydrate ($EuCl_3 \cdot 6H_2O$) were purchased from Aladdin company. Sodium acetate trihydrate ($AcONa \cdot 3H_2O$), hydroquinone dimethyl, hydroquinone, and ethyl bromoacetate were purchased from the Energy Chemical company. Zebrafishes were obtained from Nanjing EzeRinka Biotechnology Co., Ltd. Limnodilus and cabbage seeds were gained as gifts from the College of Plant Science, Jilin University. ^1H NMR spectra were collected on a Bruker AVANCE III 300 MHz NMR spectrometer. Electrospray mass spectrometric analysis (ESI-MS) was performed on a Bruker Agilent1290-microTOF Q II Mass Spectrometer. UV-vis and fluorescence spectra were collected on Shimadzu UV-2550 and Shimadzu RF-5301PC spectrometers, respectively. X-ray diffraction (XRD) measurements were carried out using a PANalytical B.V. Empyrean powder diffractometer. Fourier transform infrared (FT-IR) spectra were recorded on a Vertex 80 V spectrometer. Scanning electron microscope (SEM) and energy dispersive X-Ray spectroscopy (EDX) images were collected on a HITACHI SU8082 instrument. Thermogravimetric analysis (TGA) was performed under an air atmosphere with a heating rate of 10 ºC/min by using a NETZSCH STA499F3 QMS403D thermogravimetric analyzer. Carbon dioxide-sorption analysis was performed on a Micromeritics 3Flex analyzer. The specific surface area was calculated from the adsorption branch using Brunauer-Emmett-Teller (BET) method.

2. Syntheses and Methods

Synthesis of P1: The synthetic routes to P1 and the following compounds were shown in Figures S1 and S17. P1 was synthesized according to the published procedures.[S1-S3]

Synthesis of P2: P1 (1 g, 1.33 mmol) was dissolved in CH_2Cl_2 (100 mL) and an aqueous solution of $(NH_4)_2[Ce(NO_3)_6]$ (1.46 g, 2.66 mmol) was added dropwise at room temperature. After the mixture was reacted for 1 h, the organic layer was collected and purified by column chromatography on silica gel (light petroleum : dichloromethane : ethyl acetate, v : v, 20:10:1) to give the final product.[S4] Yield: 325.7 mg, 34.0%. ^1H NMR (300 MHz, $CDCl_3$): 6.84 (s, 2H), 6.81 (s, 2H), 6.80 (s, 2H), 6.67 (d, 4H), 3.79 (d, 6H), 3.75 (s, 6H), 3.72 (d, 12H), 3.63 (s, 6H), 3.59 (s, 4H).

Synthesis of P3: The aqueous solution of $Na_2S_2O_4$ (14.4 g, 83.4 mmol) was added dropwise into the solution of P2 (3 g, 4.2 mmol) in CH_2Cl_2. The reaction mixture was stirred under N_2 protection for 12 h at r.t.. After the solution turned white, organic phase was collected and concentrated by rotary evaporation to give the pure product. Yield: 2.3 g, 76.5 %. ^{1}H NMR (300 MHz, $CDCl_3$): 7.17 (s, 2H), 6.90 (s, 2H), 6.84 (s, 2H), 6.81 (s, 2H), 6.61 (s, 2H), 6.59 (s, 2H), 3.84 (s, 6H), 3.77 (s, 12H), 3.74 (s, 6H), 3.69 (s, 6H), 3.68 (s, 4H).

Synthesis of P4: P3 (200 mg, 0.28 mmol) was dissolved in a mixture of CH_3CN (30 mL), K_2CO_3 (300 mg, 2.2 mmol), and catalytic amount of KI and protected by N_2 atmosphere. After the reaction mixture was stirred for 30 min, ethyl bromoacetate (0.25 mL, 2.3 mmol) was injected into the system and the mixture was heated at reflux for 3 days. Finally, the crude product was purified by crystallization process, that is, by adding pour cyclohexane slowly into the CH_3Cl solution of the product. Yield: 96.4 mg, 38.5%. ^{1}H NMR (300 MHz, $CDCl_3$): 6.85 (d, 4H), 6.84 (s, 2H), 6.78 (s, 2H), 6.71 (s, 2H), 4.55 (s, 4H), 3.75 (s, 15H), 3.73 (s, 6H), 3.70 (s, 6H), 3.68 (s, 6H), 3.64 (s, 1H), 3.15-3.13 (q, 4H).

Synthesis of DCP5: A solution of P4 (200 mg, 0.22 mmol) was dissolved in tetrahydrofuran (THF, 20 mL), followed by the gradual addition of NaOH (176 mg, 4.4 mmol) solution (10 mL). The mixture was heated at reflux overnight under N_2 atmosphere. The organic phase was concentrated, followed by the addition of deionized water for dilution, then HCl was gradually added into the former solution to produce solid precipitate. After centrifugation and washing the solid by deionized water for 3 times, DCP5 was obtained.[S5] Yield: 126.9 mg, 68.8%. ^{1}H NMR (300 MHz, $CDCl_3$): 6.82 (s, 4H), 6.79 (s, 2H), 6.69 (s, 2H), 6.64 (s, 2H), 4.54 (s, 4H), 3.82 (s, 4H), 3.77 (s, 6H), 3.71 (s, 12H), 3.68 (d, 12H).

Synthesis of 1,4-Phenylenedioxydiethyl acetate (PDDE): K_2CO_3 (13.8 g, 100 mmol) and KI (20 mg) were added into the solution of hydroquinone (2.0 g, 18.2 mmol) in CH_3CN (50 mL) under N_2 protection. After stirred the mixture for 30 min, ethyl bromoacetate (1.32 mL, 109.2 mmol) was injected into the mixture which was heated at reflux for another 3 days. Finally, the crude product was concentrated and purified by recrystallization from its mixed solution of $CHCl_3$ and cyclohexane. Yield: 2.0 g, 38.8%. ^{1}H NMR (300 MHz, $CDCl_3$): 6.86 (s, 2H), 4.68 (s, 1H), 4.57 (s, 2H), 4.30-4.23 (m, 4H), 1.56 (s, 1H), 1.32-1.27 (m, 6H).

Synthesis of PDDA: NaOH (2.8 g, 70 mmol) solution was added into the solution of PDDE (1 g, 3.5 mmol) in THF (30 mL) followed by heating at reflux overnight. Afterward, the organic layer was concentrated and the obtained mixture containing the crude was diluted by deionized water. Crude solid appeared after acidifying the former solution with HCl. Finally, the crude product was washed by deionized water to give the pure PDDA.[S6] Yield: 754.5 mg, 95.4%. ^{1}H NMR (300 MHz, DMSO-*d6*): 12.93 (s, 2H), 6.83 (s, 4H), 4.59 (s, 4H).

Synthesis of PDDA-Eu_1Tb_3: The preparation method was the same as that of DCP5-Eu_xTb_y. DCM (0.05 mmol, 11.3 mg), $EuCl_3{\cdot}6H_2O$ (0.0125 mmol, 4.58 mg) and $TbCl_3{\cdot}6H_2O$ (0.0375 mmol, 14.4 mg) were dissolved in DMF (10 mL) and reacted at 150 °C for 24 h to give the control polymer DCM-Eu_1Tb_3.

HR-MS (ESI) measurement of NB and 2-NA in cabbage extract mixture: The cabbage extract mixture (1 μL) of NB and 2-NA group was diluted with methanol solution (1 mL), respectively, for further measurement. The obtained data was as follows: For NB, HR-MS (ESI) m/z: $[M + Na + H]^+$ calcd for $C_6H_5NO_2$, 147.0246; found, 147.0762; For 2-NA, HR-MS (ESI) m/z: $[M - H]^+$ calcd for $C_6H_6N_2O_2$, 137.0346; found, 137.0451.

3. Supporting Tables and Figures

Table S1. Comparison between the DCP5-Eu_xTb_y and previous reported macrocycle-based sensors.

Ref.	Name	Emission color	Constitute		Application
			Macrocycle	Other component	
This work	DCP5-Eu_xTb_y	Color tunable (including white color)	Dicarboxylatopillar[5]arene	Eu^{3+} and Tb^{3+}	Detect nitroaromatic pollutants (in vitro and in vivo)
S7	G1 ⊂ H1	Only blue	[2]Biphenylextended pillar[6]arene (H1)	Tetraphenylethylene bridged bis(quaternary ammonium) (G1)	Detect Hg^{2+} (In vitro)
S8	TPE-Q4 ⊂ DSP5	Only blue	Disulfonated pillar[5]arene (DSP5)	TPE-based tetratopic guest (TPE-Q4)	Detect Fe^{3+} (In vitro)
S9	P[5]-TPE-CMP	Only green	Pillar[5]arene (P[5])	1,1,2,2-Tetrakis(4-ethynylphenyl)ethane (TPE)	Detect Fe^{3+} (In vitro)
S10	SOF (comprised of TPE-4MV,	Only green	Cucurbit[8]uril (CB[8])	Viologen derivative (TPE-4MV) and azobenzene derivative (AZO)	Detect azoreductase in Escherichia coli

	CB[8], and AZO)				
S11	6CD-Ru	Only red	Cyclodextrins (CD)	--	Detect lysozyme (In vitro)
S12	G2 ⊂ P5-TPE	Only yellow	TPE-containing conjugated polymer with pendent pillar[5]arene units (P5-TPE)	Symmetric BB type crosslinker (G2)	Detect explosive (In vitro)
S13	MCx-1	Only yellow	Merocyanine calixarene (MCx-1)	--	Detect methyltransferase (In vitro)
S14	CB7-TO	Only white	Cucurbit[7]uril (CB7)	Thiazole orange (TO)	Detect Na^+ and Ca^{2+} (In vitro)

Table S2. CIE coordinates of DCP5-Eu_1Tb_1 at different excitation wavelengths.

Excitation wavelength	300 nm	310 nm	320 nm	330 nm	340 nm
CIE coordinate	(0.21, 0.18)	(0.21, 0.18)	(0.22, 0.19)	(0.25, 0.22)	(0.33, 0.27)
	350 nm	360 nm	370 nm	380 nm	
	(0.43, 0.28)	(0.51, 0.27)	(0.57, 0.29)	(0.57, 0.33)	

Table S3. CIE coordinates of DCP5-Eu_xTb_y with varying molar ratios of Eu^{3+} : Tb^{3+} at 340 nm excitation.

Molar ratio of Eu^{3+} : Tb^{3+}	1 : 0	3 : 1	1 : 1	1 : 3	0 : 1
	DCP5-Eu	DCP5-Eu_3Tb_1	DCP5-Eu_1Tb_1	DCP5-Eu_1Tb_3	DCP5-Tb
CIE coordinate	(0.32, 0.26)	(0.32, 0.28)	(0.33, 0.27)	(0.31, 0.31)	(0.28, 0.32)

Table S4. Life times of DCP5-Eu_1Tb_3 at different emission wavelengths.

	λ_{em}	τ_1	τ_2	τ	χ^2
DCP5-Eu_1Tb_3	430 nm	1.14 ns (54.90%)	8.98 ns (45.10%)	4.68 ns	1.318
	546 nm	0.10 ms (30.75%)	1.26 ms (69.25%)	0.90 ms	1.784
	619 nm	0.35 ms (49.25%)	1.19 ms (50.75%)	0.78 ms	1.158

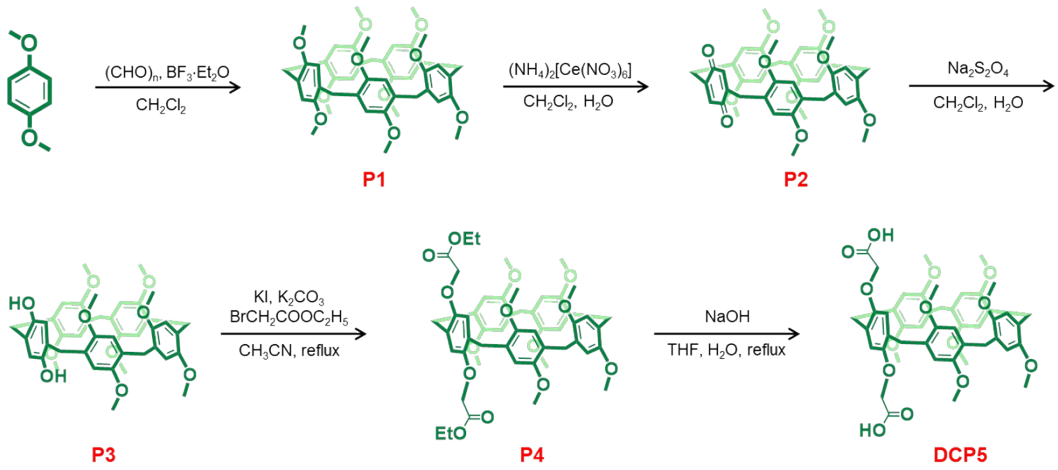

Figure S1. Synthetic route to DCP5.

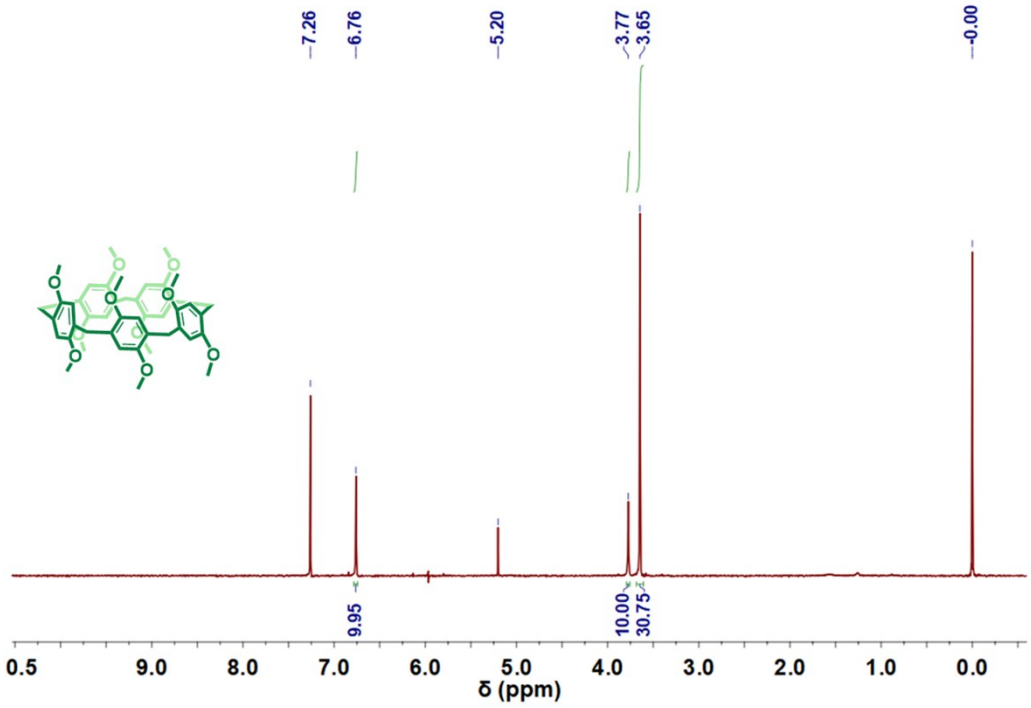

Figure S2. ^{1}H NMR (300 MHz, $CDCl_3$, 298K) spectrum of P1.

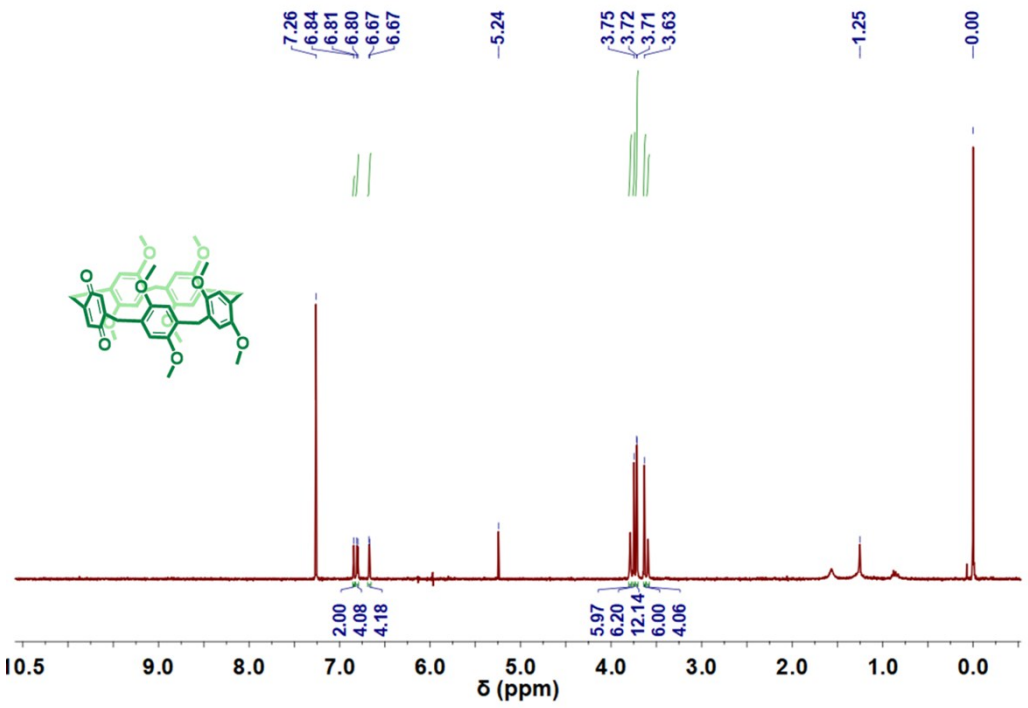

Figure S3. ^{1}H NMR (300 MHz, $CDCl_3$, 298K) spectrum of P2.

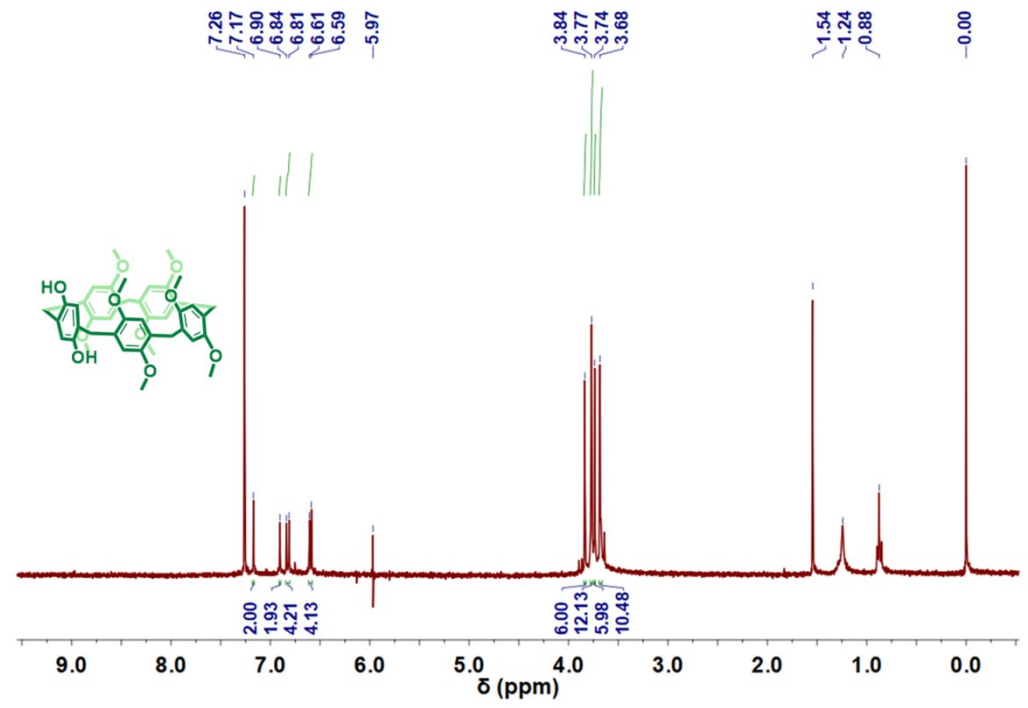

Figure S4. ^{1}H NMR (300 MHz, $CDCl_3$, 298K) spectrum of P3.

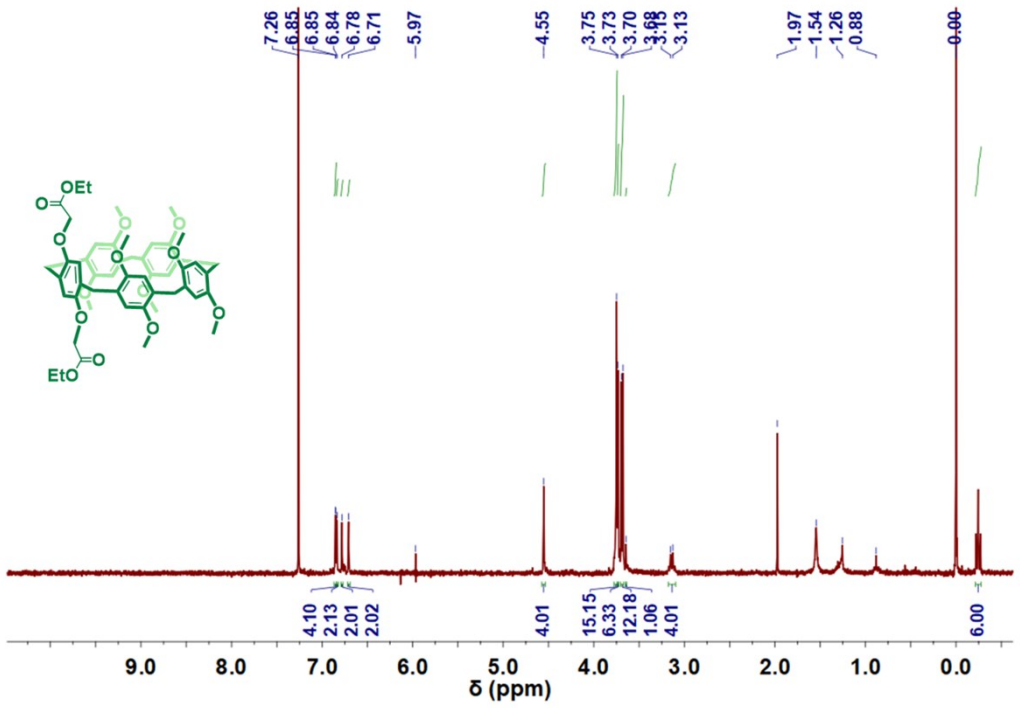

Figure S5. ^{1}H NMR (300 MHz, $CDCl_3$, 298K) spectrum of P4.

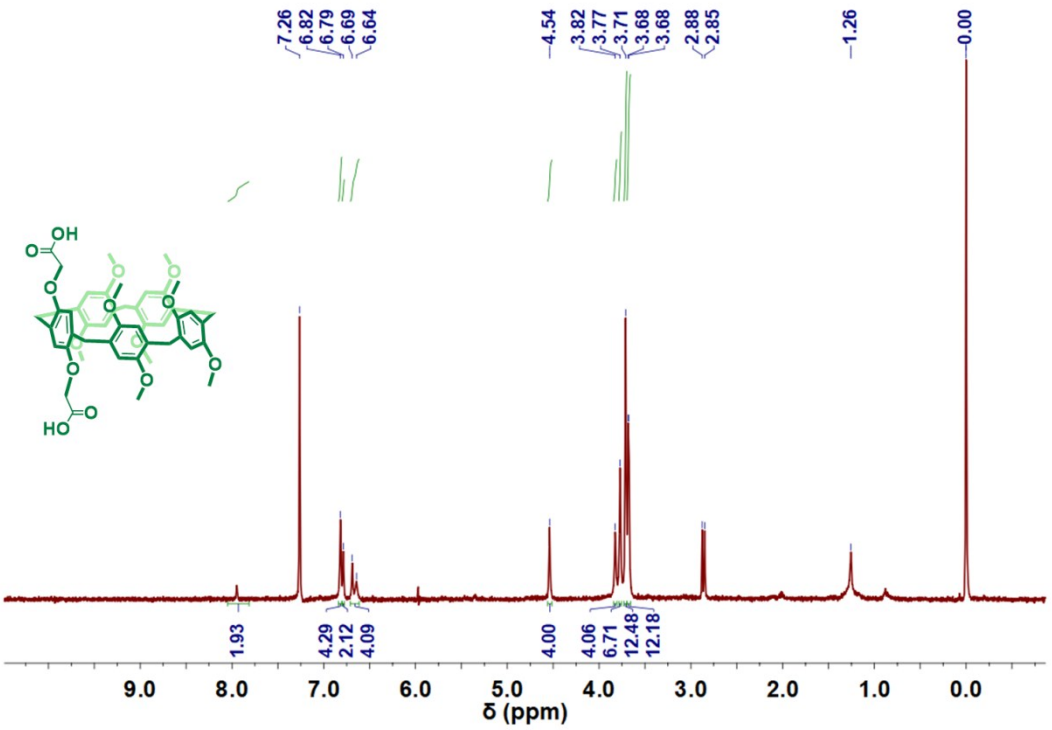

Figure S6. ^{1}H NMR (300 MHz, $CDCl_3$, 298K) spectrum of DCP5.

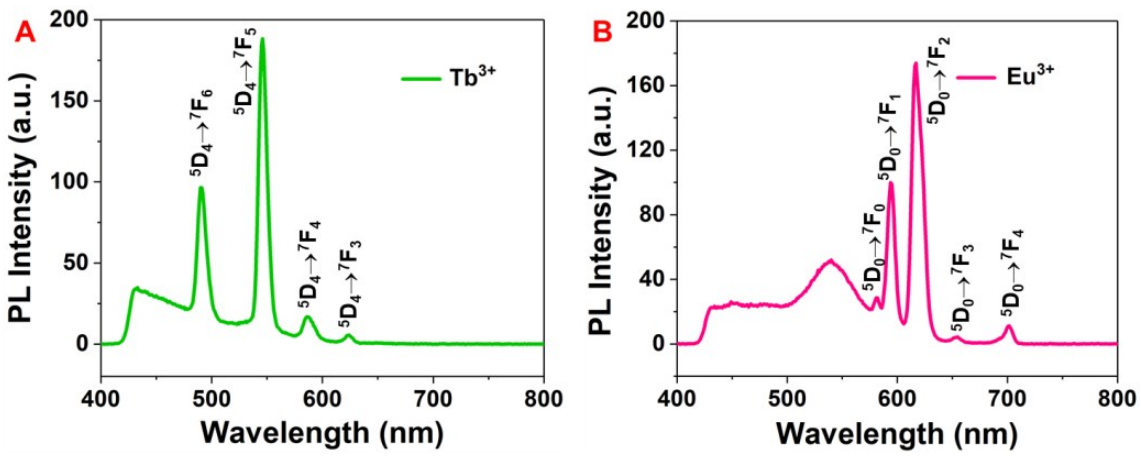

Figure S7. Fluorescence emission spectra of free (A) Tb^{3+} and (B) Eu^{3+} at the excitation wavelength of 280 nm. (Slit width: ex = 10 nm, em = 5 nm)

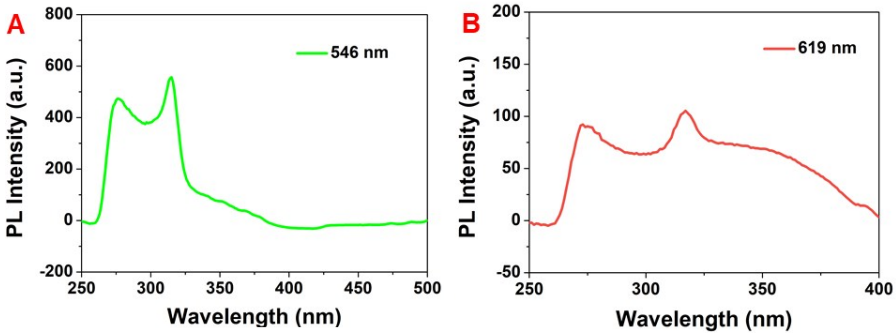

Figure S8. Excitation spectrum of DCP5-Eu_1Tb_3 in DMF at the emission wavelength of (A) 545 nm and (B) 619 nm, respectively. (Slit width: ex = 10 nm, em = 5 nm)

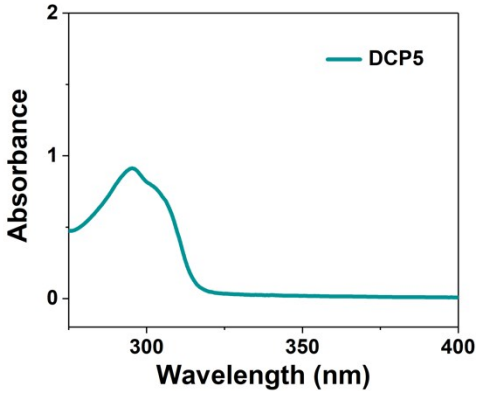

Figure S9. UV-vis spectrum of DCP5.

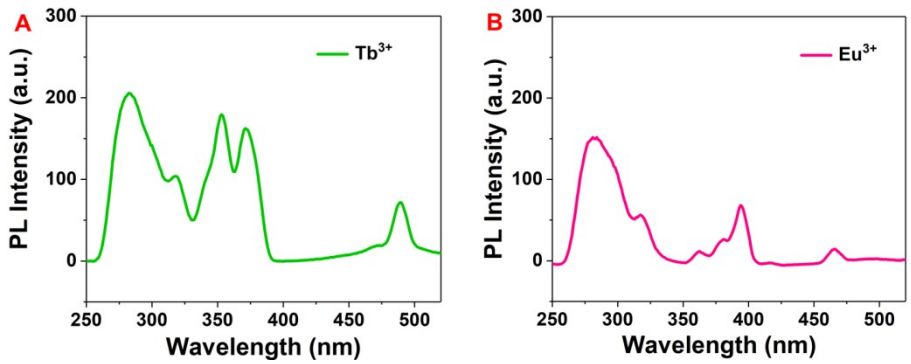

Figure S10. Excitation spectrum of free (A) Tb^{3+} (monitored at 546 nm) and (B) Eu^{3+} (monitored at 619 nm). (Slit width: ex = 10 nm, em = 5 nm)

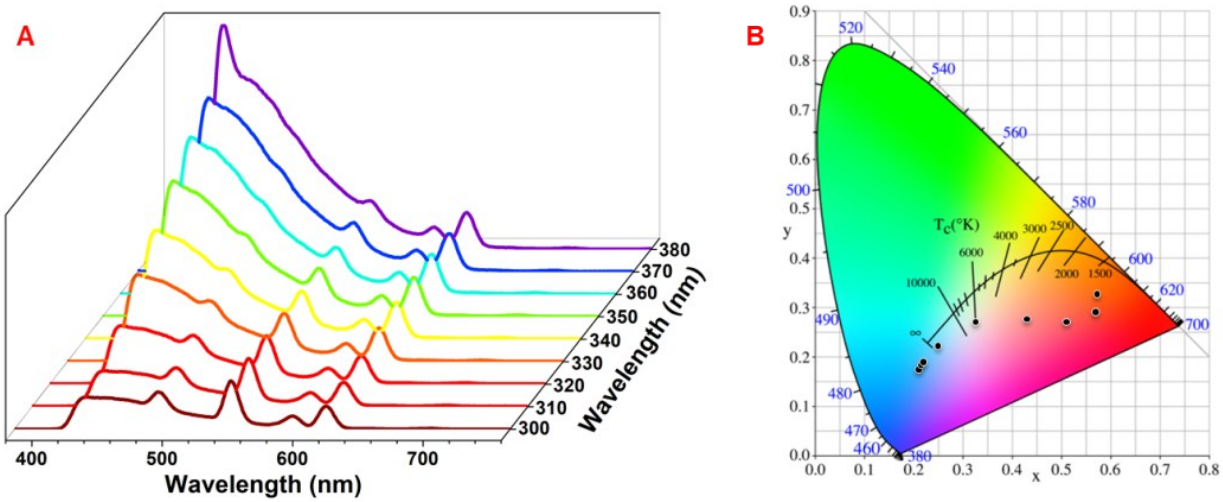

Figure S11. (A) Fluorescence spectra and (B) CIE coordinate of DCP5-Eu_1Tb_1 in DMF at the excitation wavelengths from 300 nm to 380 nm. (Slit width: ex = 10 nm, em = 5 nm)

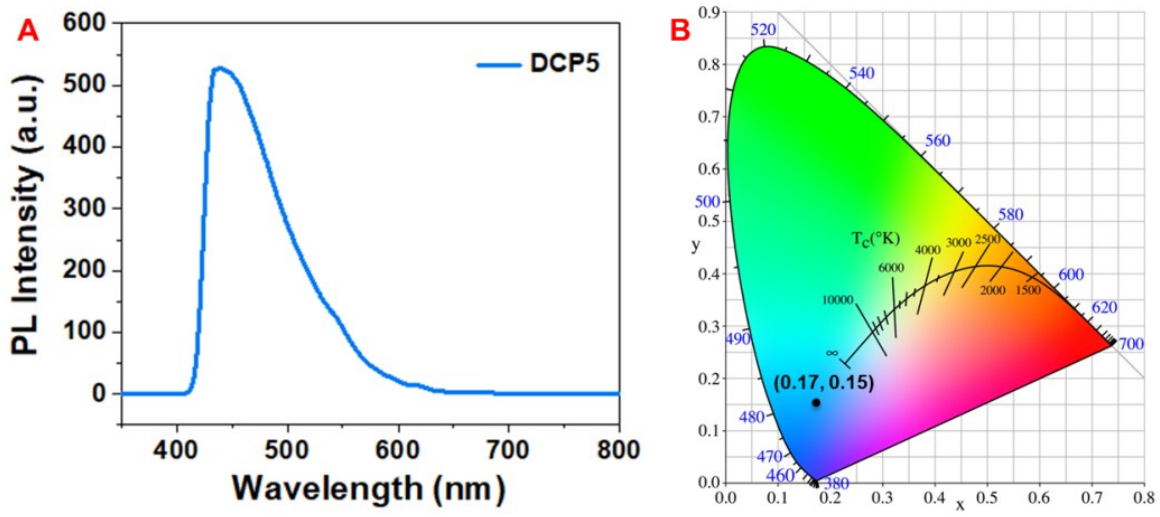

Figure S12. (A) Fluorescence spectrum and (B) CIE coordinate of DCP5 ligand in DMF. (Slit width: ex = 10 nm, em = 5 nm, λ_{ex} = 340 nm)

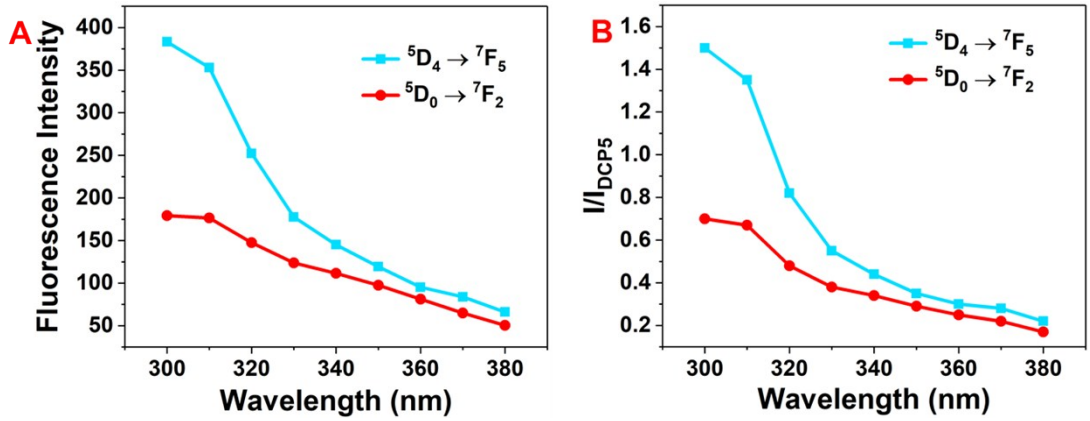

Figure S13. (A) Fluorescence intensity of $^5D_4 \rightarrow {}^7F_5$ transition of Tb^{3+} at 546 nm and $^5D_0 \rightarrow {}^7F_2$ transition of Eu^{3+} at 619 nm in DCP5-Eu_1Tb_1 under different excitation wavelengths. (B) Ratio plot of the fluorescence intensity of $^5D_4 \rightarrow {}^7F_5$ transition of Tb^{3+} at 546 nm and $^5D_0 \rightarrow {}^7F_2$ transition of Eu^{3+} at 619 nm versus the fluorescence intensity of DCP5 at 430 nm in DCP5-Eu_1Tb_1 under different excitation wavelengths (I represents the fluorescence intensity of $^5D_4 \rightarrow {}^7F_5$ or $^5D_0 \rightarrow {}^7F_2$, I_{DCP5} represents the fluorescence intensity of DCP5). (Solvent = DMF, λ_{ex} = 340 nm, slit width: ex = 10 nm, em = 5 nm)

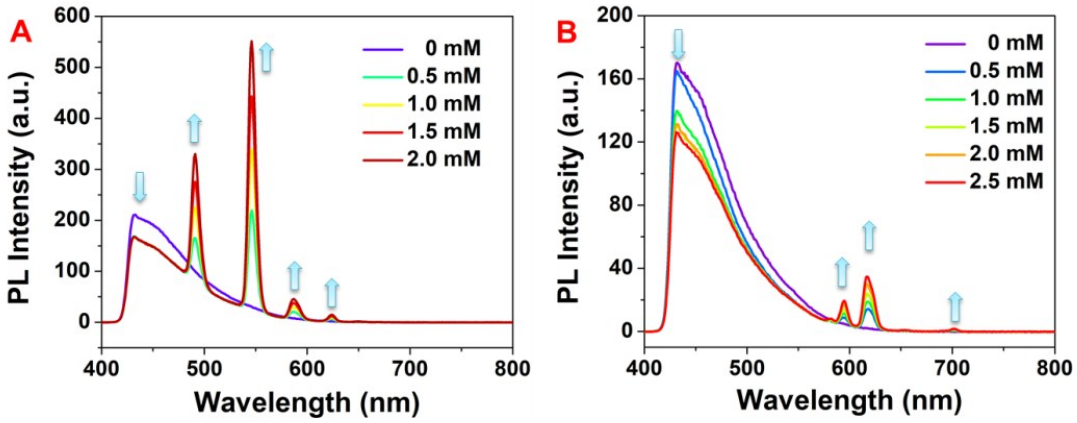

Figure S14. Emission spectra of DCP5 (0.625 mM) upon gradual titration of (A) Eu^{3+} solution and (B) Tb^{3+} solution. (Solvent = DMF, λ_{ex} = 340 nm, slit width: ex = 10 nm, em = 5 nm)

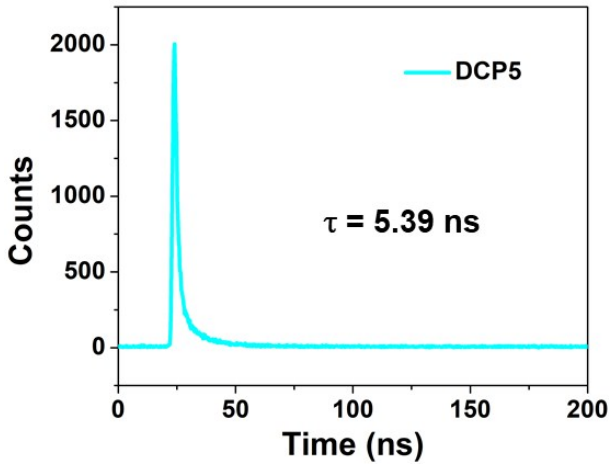

Figure S15. Time-resolved fluorescence decay curve of DCP5.

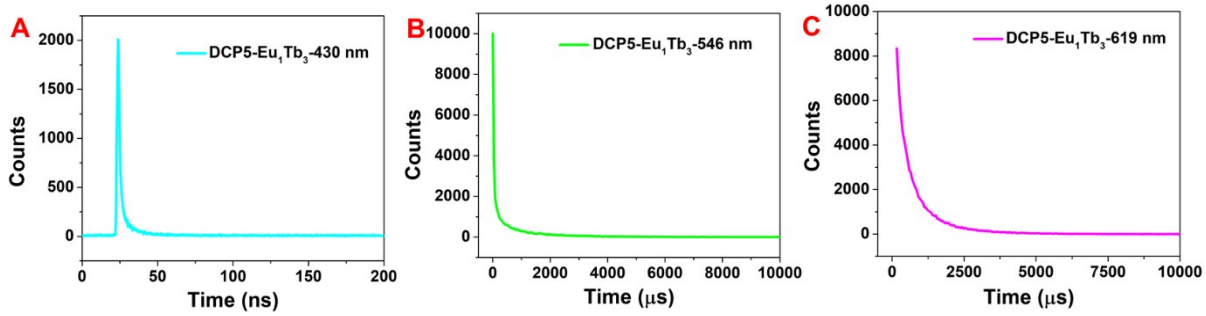

Figure S16. Time-resolved fluorescence decay curves of DCP5-Eu_1Tb_3 at different emission wavelengths: (A) 430 nm, (B) 546 nm, and (C) 619 nm.

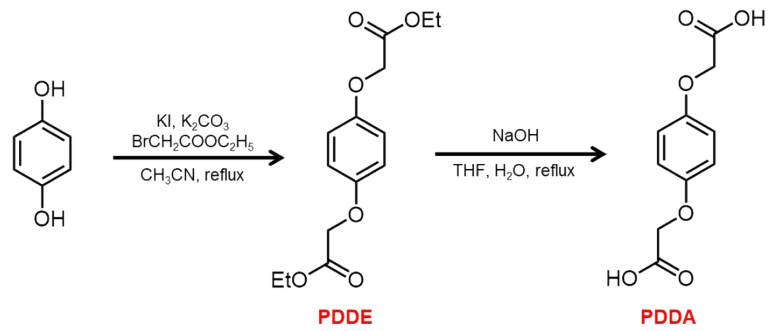

Figure S17. Synthetic route to PDDA.

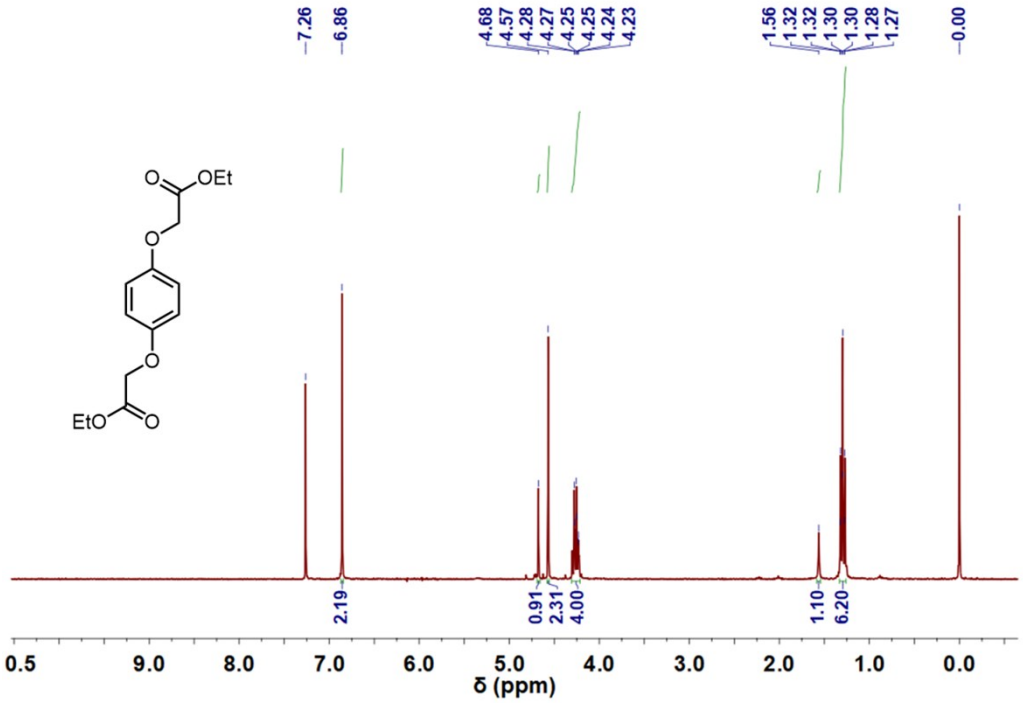

Figure S18. ^{1}H NMR (300 MHz, $CDCl_3$, 298K) spectrum of PDDE.

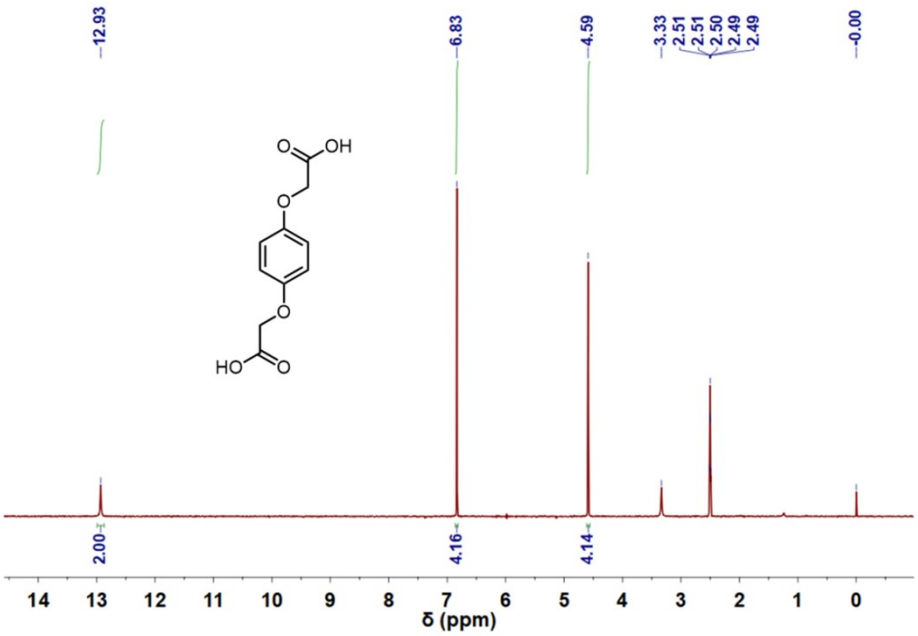

Figure S19. ^{1}H NMR (300 MHz, DMSO-*d6*, 298K) spectrum of PDDA.

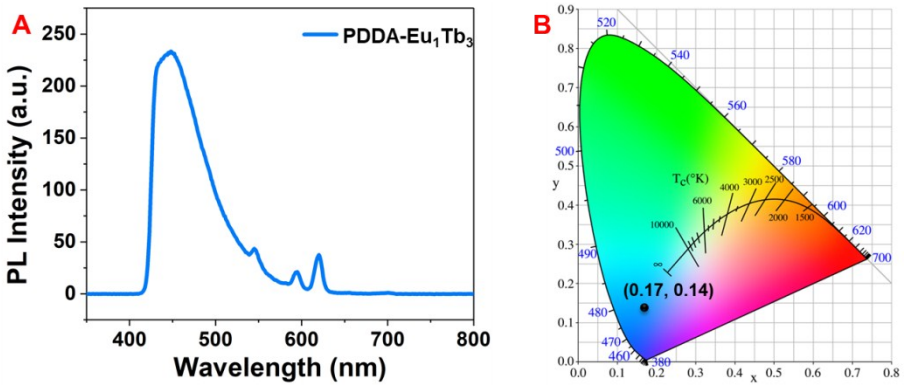

Figure S20. (A) Fluorescence spectrum and (B) CIE coordinate of DCM-Eu_1Tb_3 at 340 nm (ex.).

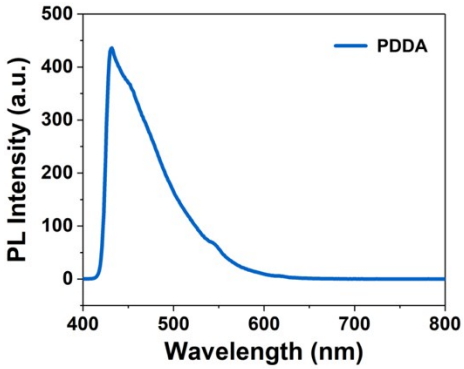

Figure S21. Fluorescence spectrum of PDDA at the excitation wavelength of 340 nm.

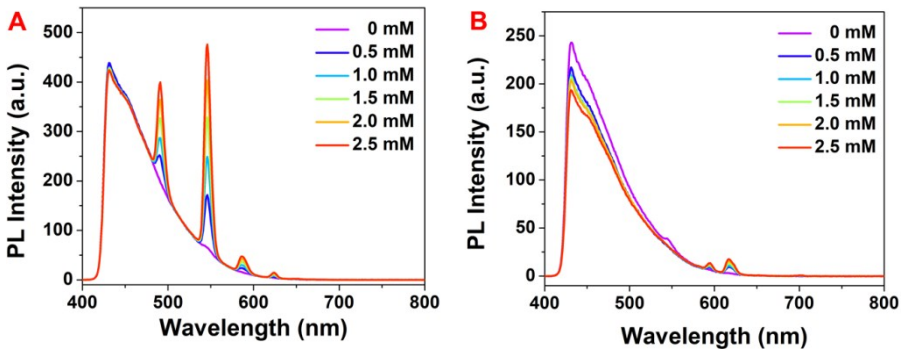

Figure S22. Emission spectra of PDDA (0.625 mM) upon gradual titration of (A) Eu^{3+} solution and (B) Tb^{3+} solution (solvent = DMF, λ_{ex} = 340 nm, slit width: ex = 10 nm, em = 5 nm).

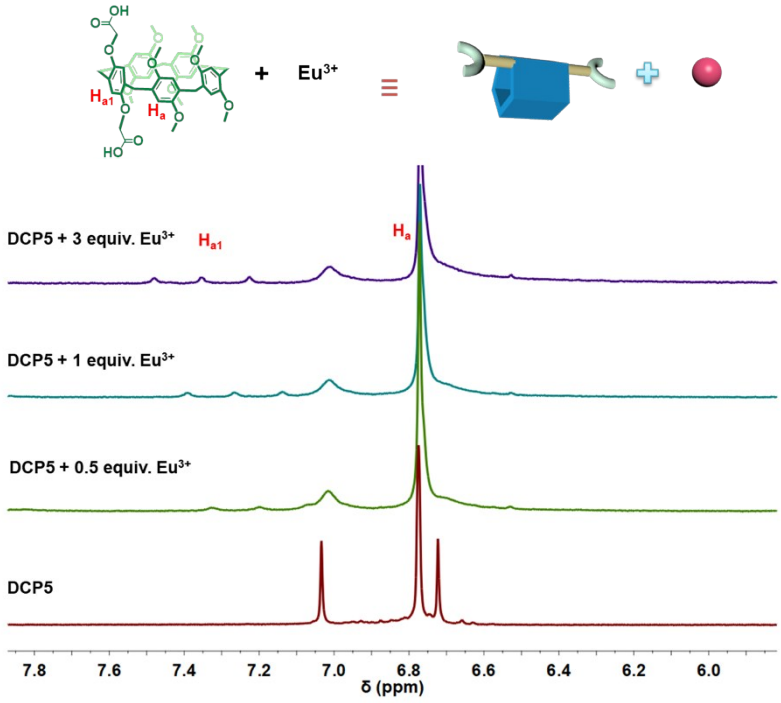

Figure S23. ^{1}H NMR spectra (400 MHz, DMSO-*d6*, 298 K) of DCP5 (5 mM) in presence of various concentrations: (a) 0 mM; (b) 2.5 mM; (c) 5 mM; (d) 15.0 mM of $EuCl_3 \cdot 6H_2O$.

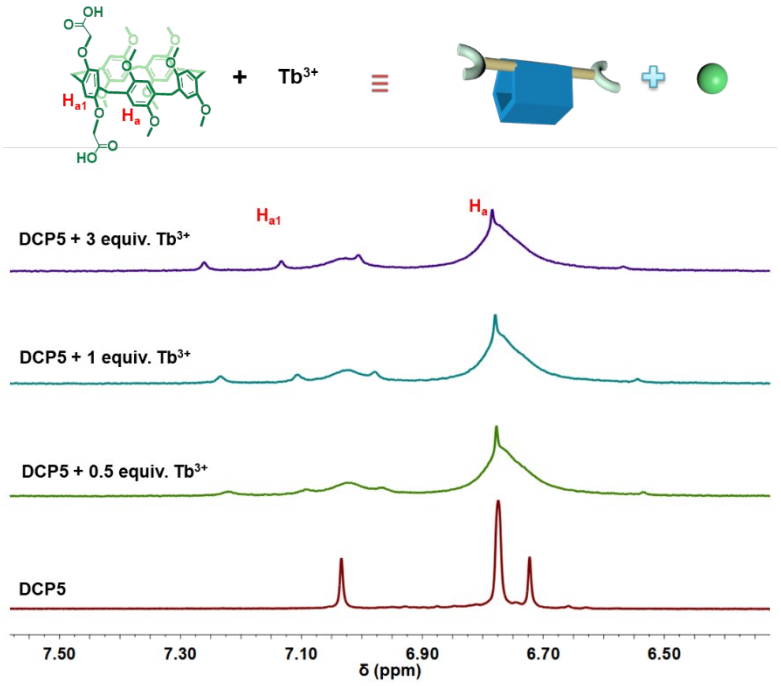

Figure S24. Partial of ^{1}H NMR spectra (400 MHz, DMSO-*d6*, 298 K) of DCP5 (5 mM) in presence of various concentrations: (a) 0 mM; (b) 2.5 mM; (c) 5 mM; (d) 15.0 mM of $TbCl_3 \cdot 6H_2O$.

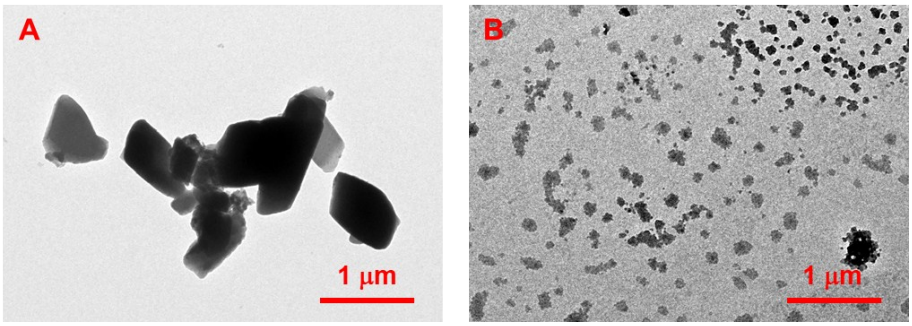

Figure S25. TEM images of DCP5-Eu_1Tb_3 and free DCP5.

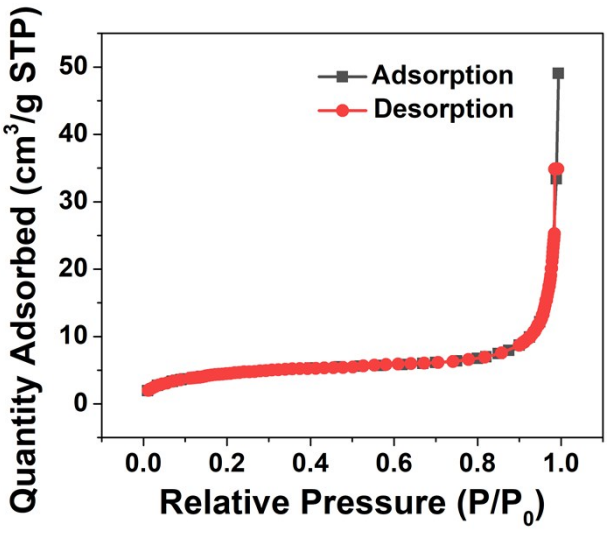

Figure S26. Nitrogen adsorption-desorption isotherms of DCP5-Eu_1Tb_3 at 298 K.

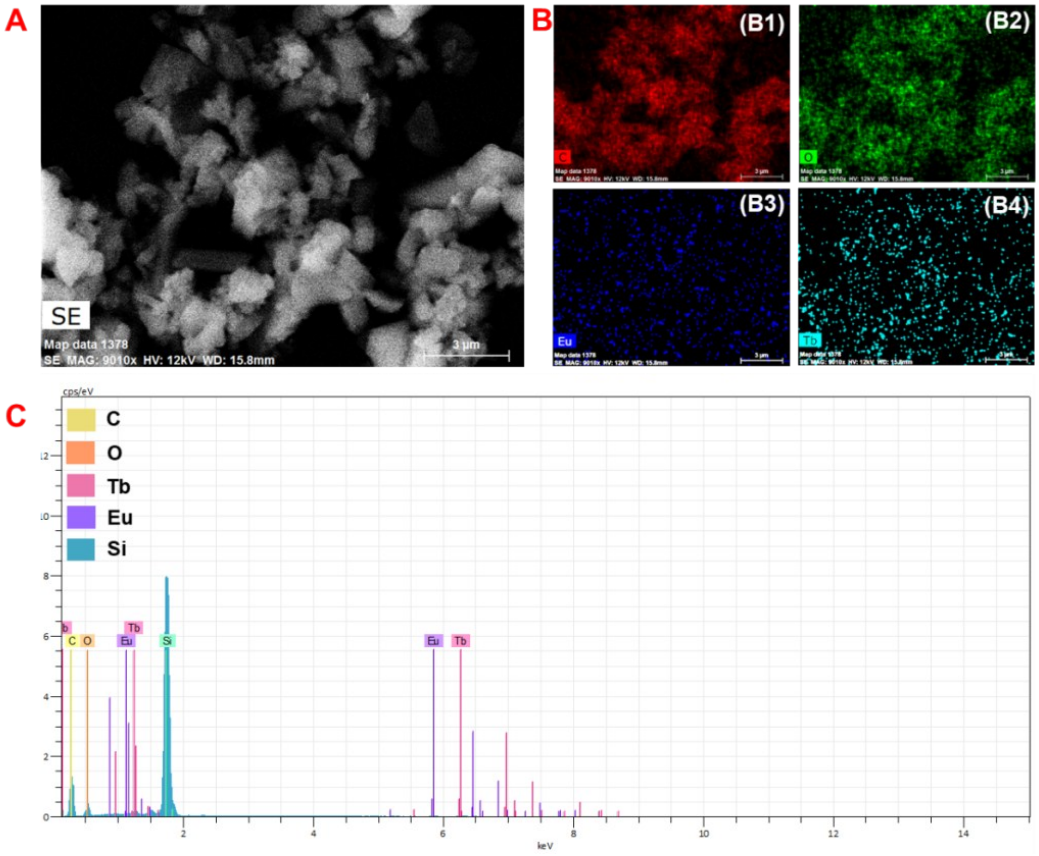

Figure S27. (A) SEM image, (B) EDX mapping images, and (C) energy spectrum of DCP5-Eu_1Tb_3.

Table S5. Molar ratio of Eu:Tb in DCP5-Eu_1Tb_3 characterized by EDX mapping.

Sample	Atomic mass ratio of Eu:Tb	Atomic mass ratio of Eu:Tb
DCP5-Eu_1Tb_3	1:2.08	1:1.99

Table S6. Molar ratio of Eu:Tb in DCP5-Eu_1Tb_3 characterized by ICP.

Sample	Concentration of Eu	Concentration of Tb	Mass ratio of Eu:Tb	Molar ratio of Eu:Tb
DCP5-Eu_1Tb_3	4.80 ppm	8.35 ppm	1:1.74	1:1.66

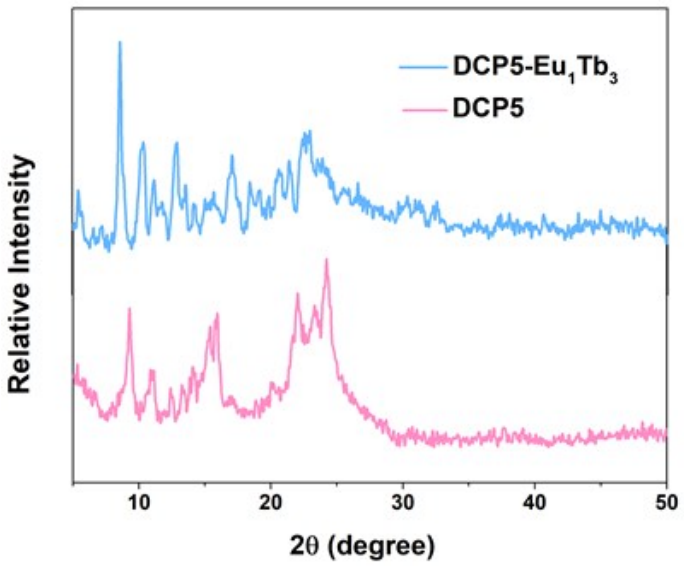

Figure S28. XRD patterns of DCP5 and DCP5-Eu_1Tb_3.

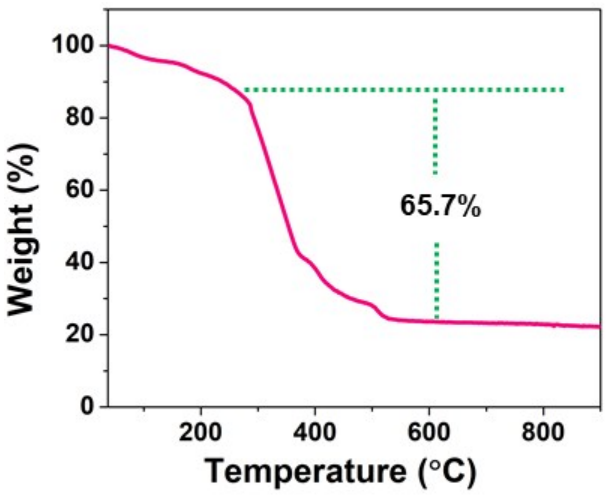

Figure S29. TGA curve of DCP5-Eu_1Tb_3.

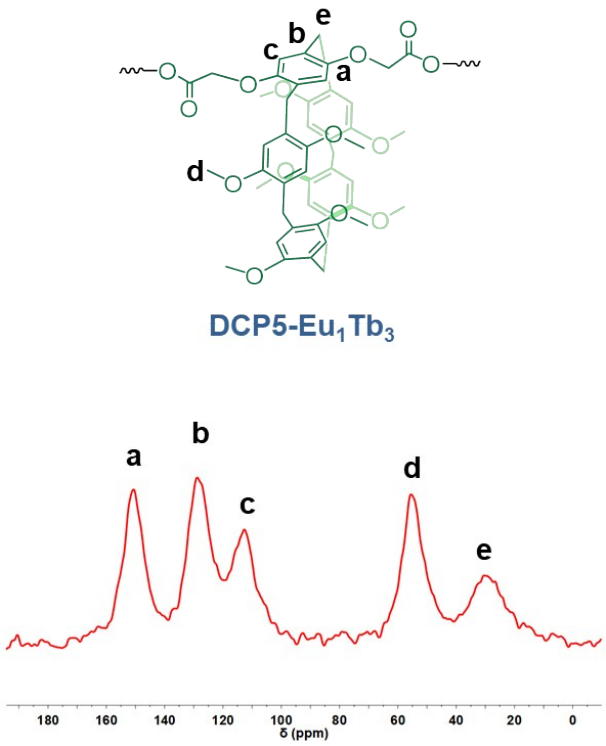

Figure S30. Solid-state CP-MAS ^{13}C NMR spectrum of DCP5-Eu_1Tb_3.

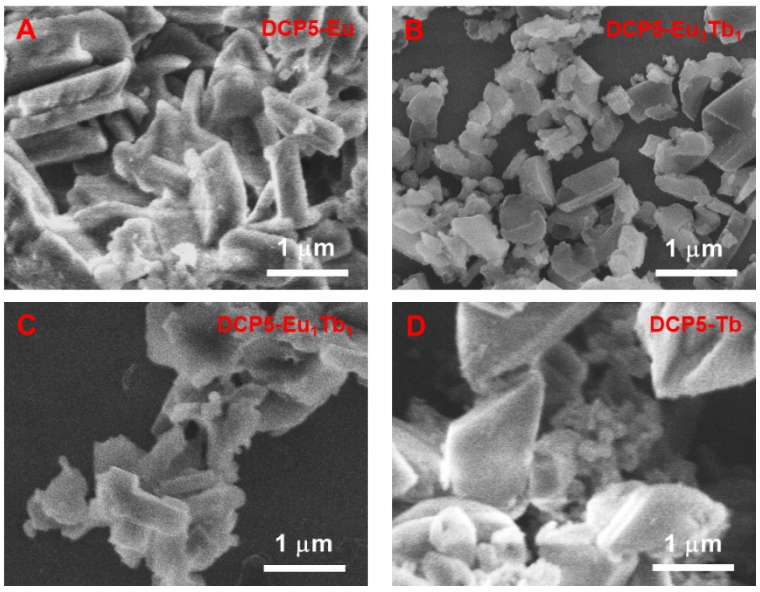

Figure S31. SEM images of (A) DCP5-Eu, (B) DCP5-Eu_3Tb_1, (C) DCP5-Eu_1Tb_1, and (D) DCP5-Tb.

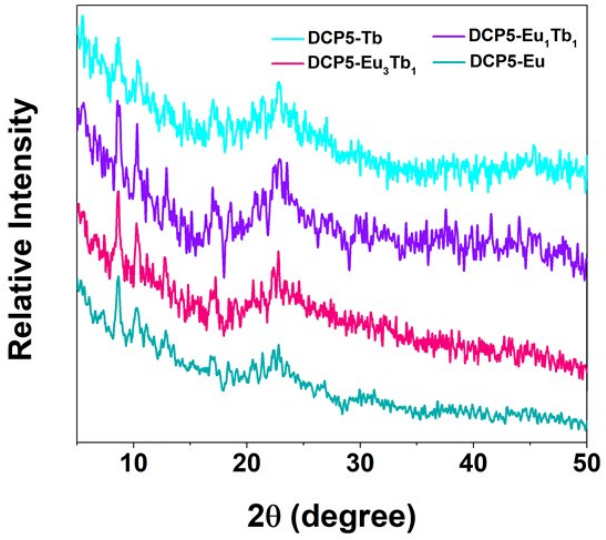

Figure S32. XRD patterns of DCP5-Eu, DCP5-Eu_3Tb_1, DCP5-Eu_1Tb_1, and DCP5-Tb.

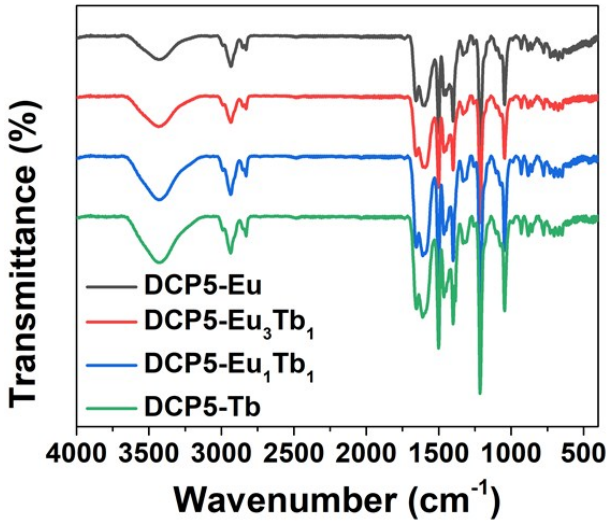

Figure S33. FT-IR spectra of DCP5-Eu, DCP5-Eu_3Tb_1, DCP5-Eu_1Tb_1, and DCP5-Tb.

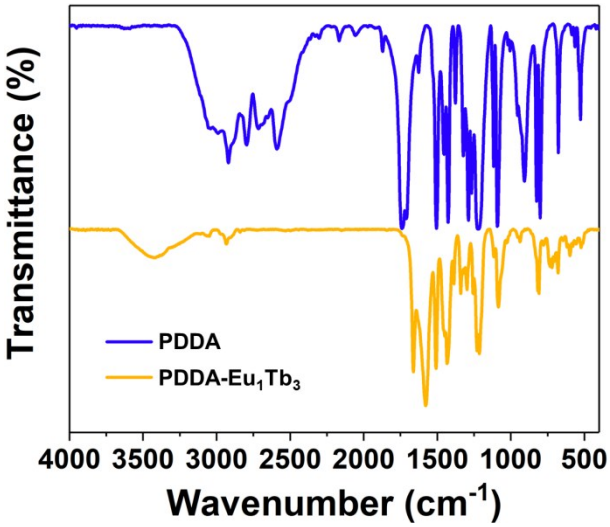

Figure S34. FT-IR spectra of PDDA and PDDA-Eu_1Tb_3.

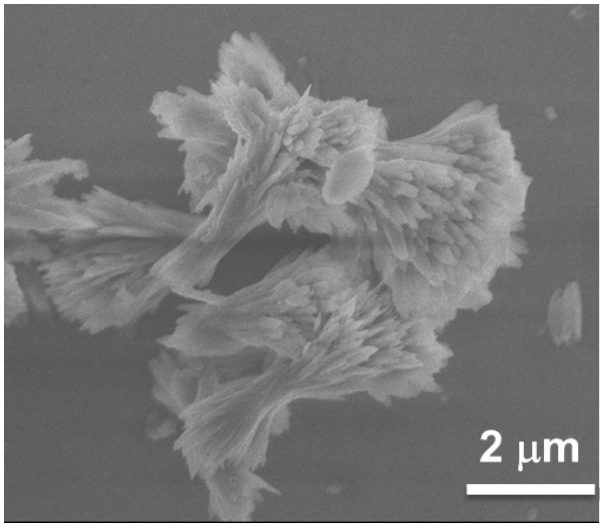

Figure S35. SEM image of PDDA-Eu_1Tb_3.

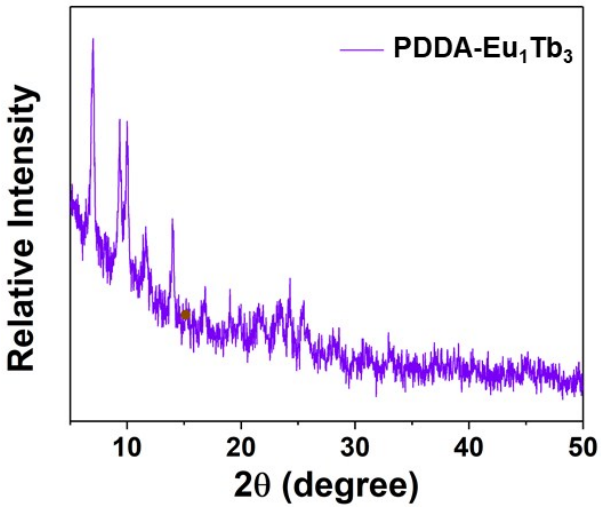

Figure S36. XRD pattern of PDDA-Eu_1Tb_3.

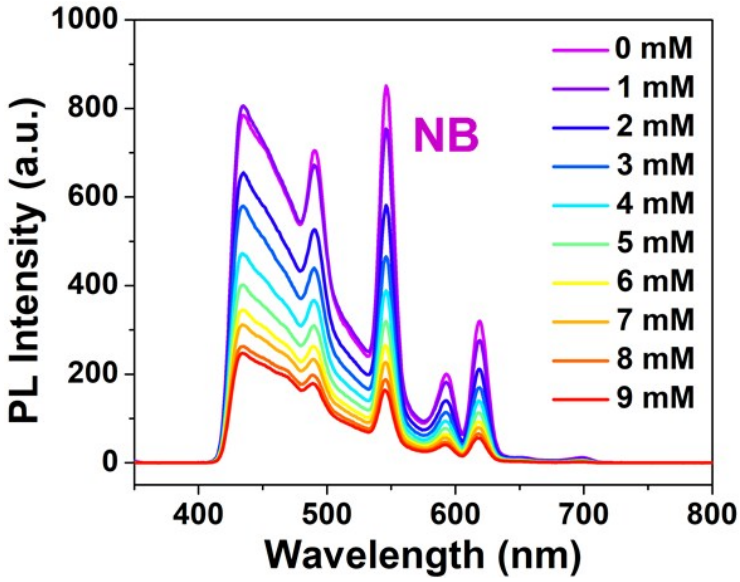

Figure S37. Fluorescence spectra of DCP5-Eu_1Tb_3 with increasing addition of NB at the excitation wavelength of 340 nm. (0.5 mg/mL, solvent = DMF, slit width: ex = 10 nm, em = 10 nm)

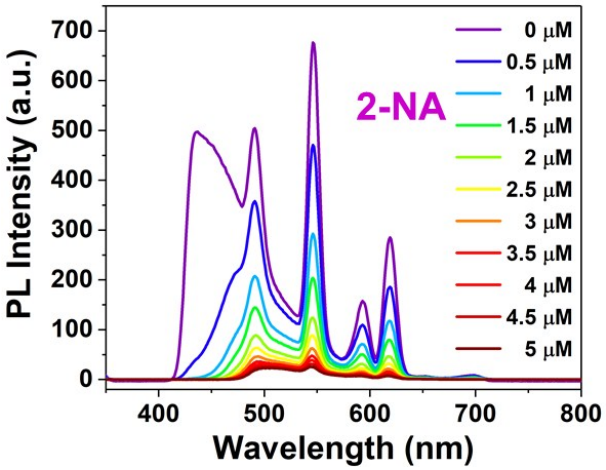

Figure S38. Fluorescence spectra of DCP5-Eu_1Tb_3 with increasing addition of 2-NA at the excitation wavelength of 340 nm. (0.2 mg/mL, solvent = DMF, slit width: ex = 10 nm, em = 10 nm)

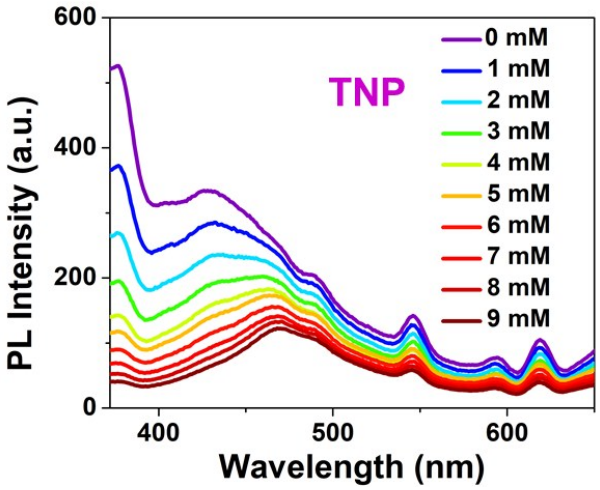

Figure S39. Fluorescence spectra of DCP5-Eu_1Tb_3 with increasing addition of TNP at the excitation wavelength of 340 nm. (0.2 mg/mL, solvent = DMF, slit width: ex = 10 nm, em = 10nm)

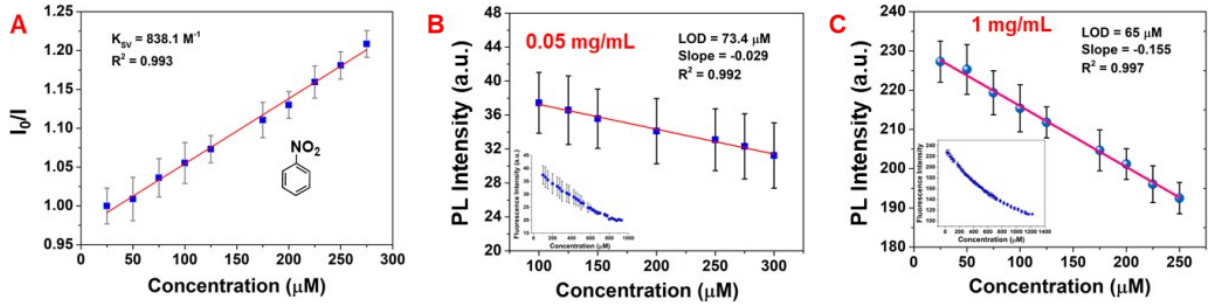

Figure S40. Plots of (A) relative fluorescence intensity of DCP5-Eu_1Tb_3 at the emission wavelength of 546 nm against the concentration of NB. Fluorescence intensity of DCP5-Eu_1Tb_3 at the emission wavelength of 546 nm against the concentration of NB with the concentration of DCP5-Eu_1Tb_3 is (B) 0.05 mg/mL and (C) 1 mg/mL respectively. Insets are the corresponding whole titration plots of fluorescence intensity of DCP5-Eu_1Tb_3 against NB concentration. (Solvent = DMF, λ_{ex} = 340 nm, slit width: ex = 10 nm, em = 5nm)

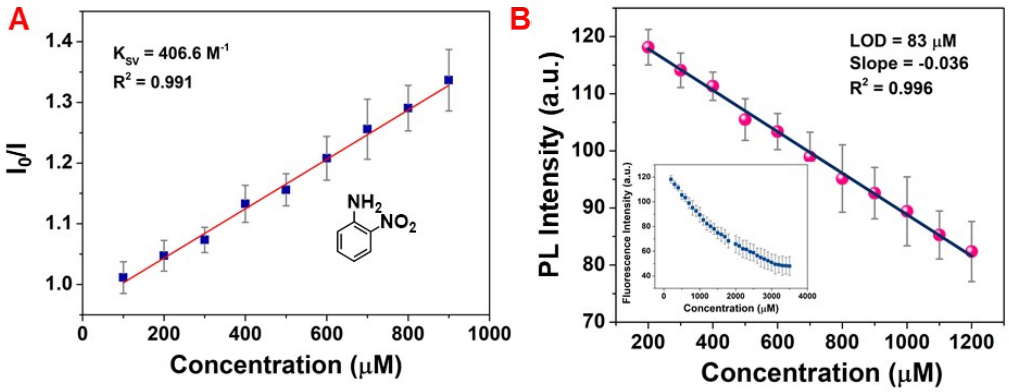

Figure S41. Plot of (A) relative fluorescence intensity and (B) fluorescence intensity of DCP5-Eu_1Tb_3 at the emission wavelength of 546 nm against the concentration of 2-NA. The inset is the whole titration plot of fluorescence intensity of DCP5-Eu_1Tb_3 against 2-NA concentration. (0.25 mg/mL, solvent = DMF, λ_{ex} = 340 nm, slit width: ex = 10 nm, em = 5nm)

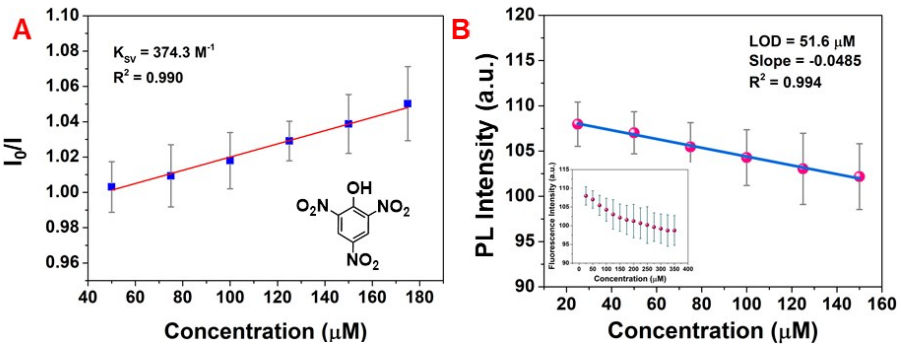

Figure S42. Plot of (A) relative fluorescence intensity and (B) fluorescence intensity of DCP5-Eu_1Tb_3 at the emission wavelength of 546 nm against the concentration of TNP. Inset is the whole titration plot of fluorescence intensity of DCP5-Eu_1Tb_3 against TNP concentration. (0.25 mg/mL, solvent = DMF, λ_{ex} = 340 nm, slit width: ex = 10 nm, em = 5 nm).

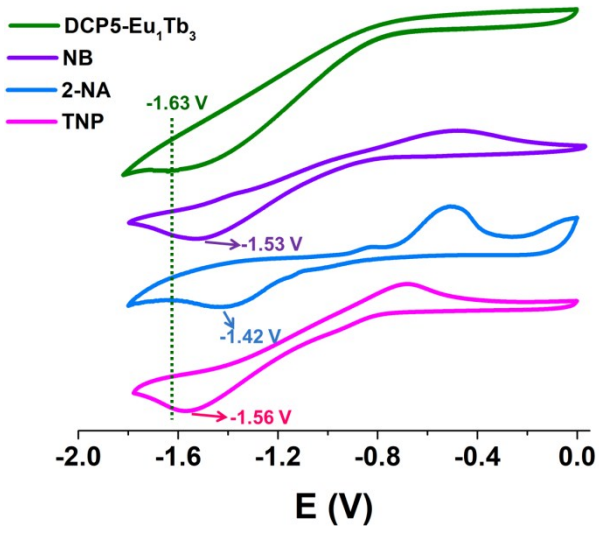

Figure S43. Cyclic voltammograms of DCP5-Eu_1Tb_3, NB, 2-NA and TNP.

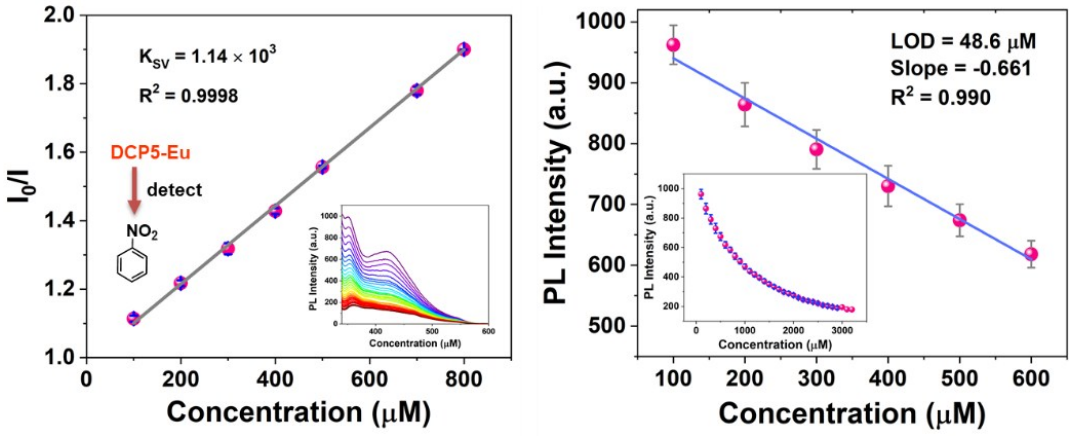

Figure S44. Plot of (A) relative fluorescence intensity and (B) fluorescence intensity of DCP5-Eu against the concentration of NB. The inset in (A) is the corresponding fluorescence spectra, and the inset in (B) is the whole titration plot of fluorescence intensity of DCP5-Eu against NB concentration. (0.25 mg/mL, solvent = DMF, λ_{ex} = 340 nm, slit width: ex = 10 nm, em = 5nm)

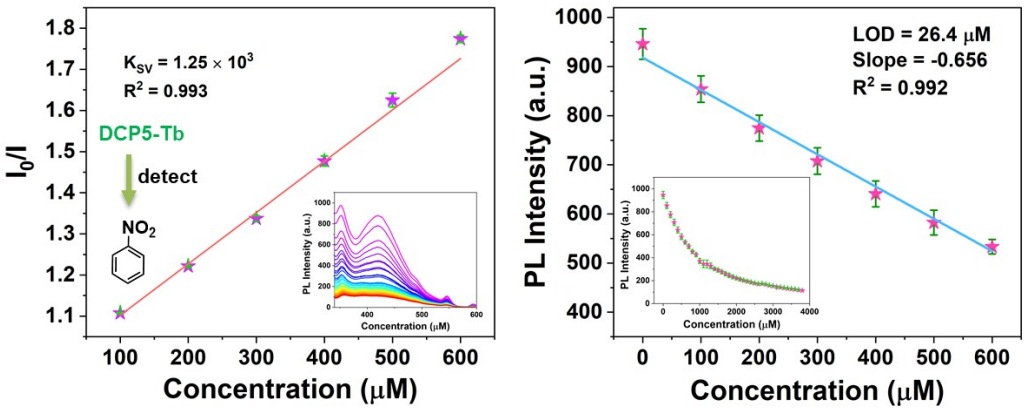

Figure S45. Plot of (A) relative fluorescence intensity and (B) fluorescence intensity of DCP5-Tb against the concentration of NB. The inset in (A) are the corresponding fluorescence spectra, and the inset in (B) is the whole titration plot of fluorescence intensity of DCP5-Tb against NB concentration. (0.25 mg/mL, solvent = DMF, λ_{ex} = 340 nm, slit width: ex = 10 nm, em = 5nm)

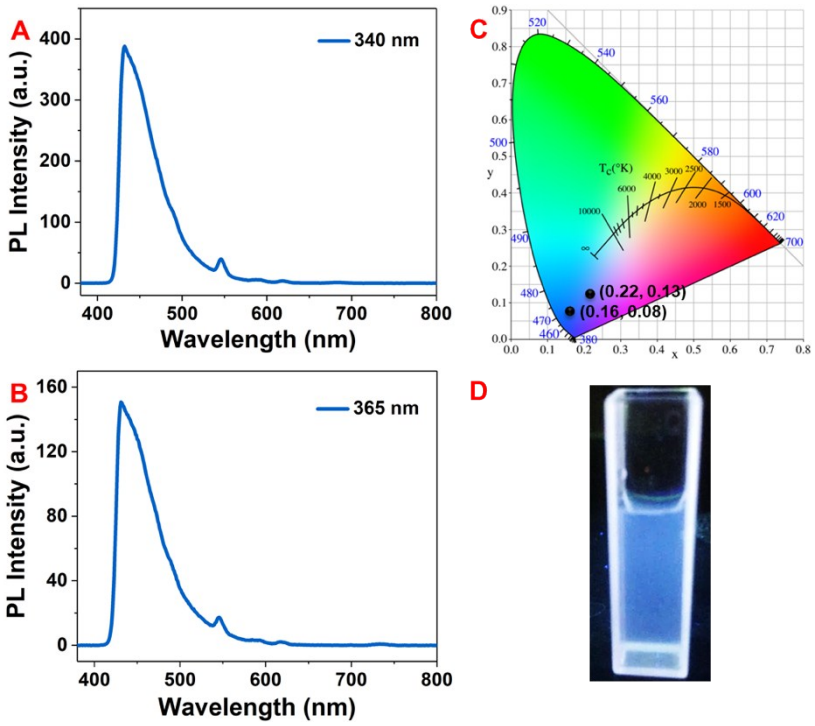

Figure S46. Fluorescence spectra of DCP5-Eu_1Tb_3 in deionized water at (A) 340 nm and (B) 365 nm, and (C) their corresponding CIE coordinates at (0.22, 0.13) and (0.16, 0.08), respectively. (0.2 mg/mL, slit width: ex = 10 nm, em = 10 nm) (D) Digital photo of DCP5-Eu_1Tb_3 in deionized water under UV light excitation.

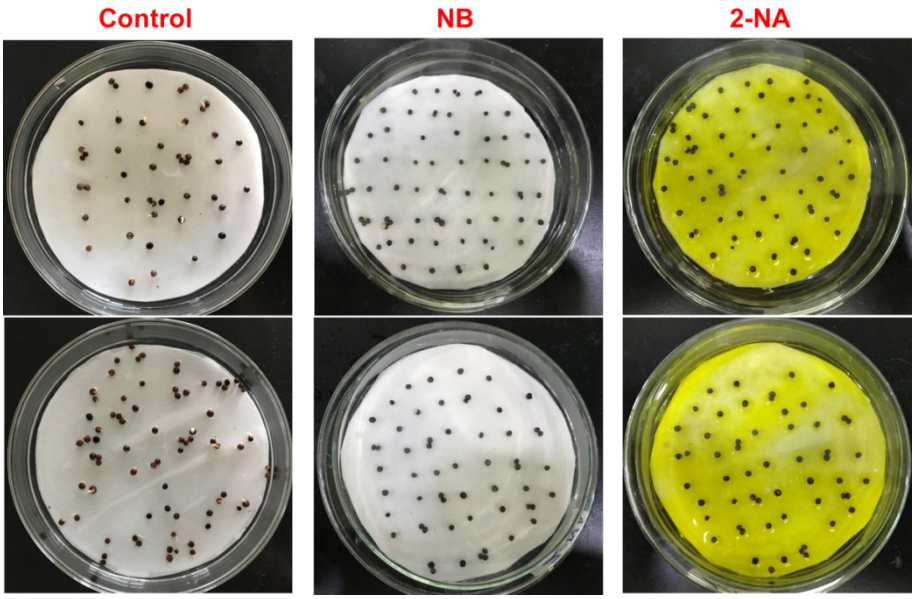

Figure S47. Digital photos of cabbage seeds treated by deionized water, NB (1 mM), and 2-NA (0.2 mM), respectively.

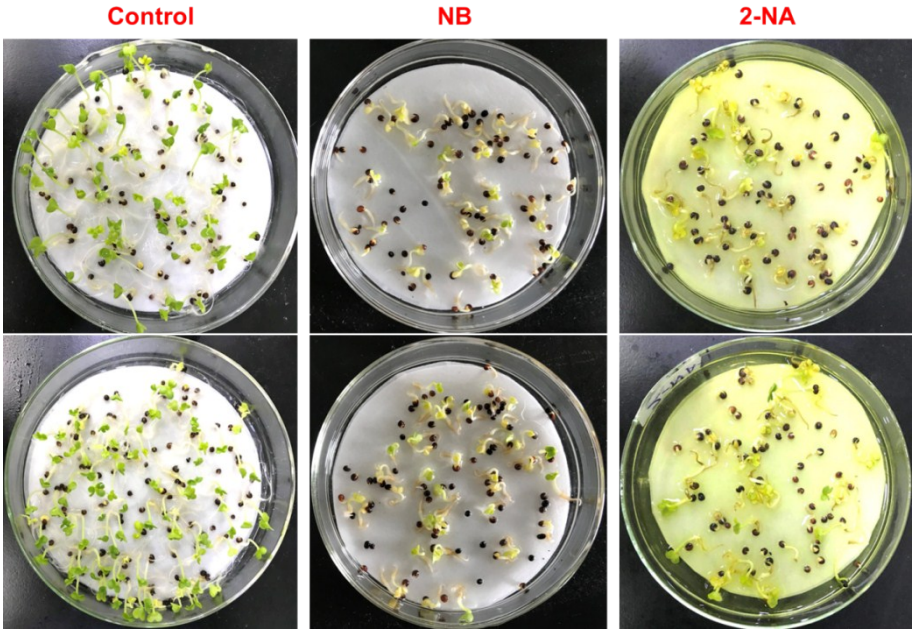

Figure S48. Digital photos of cabbages that after cultured with deionized water, NB (1 mM), and 2-NA (0.2 mM), respectively.

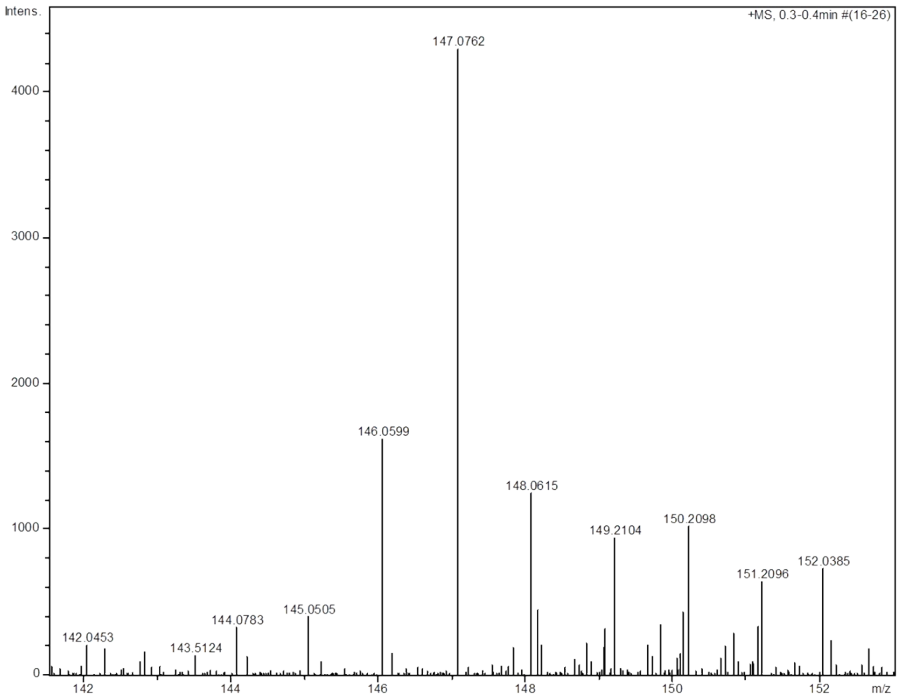

Figure S49. HR-MS (ESI) spectrum of NB in the cabbage extract mixture.

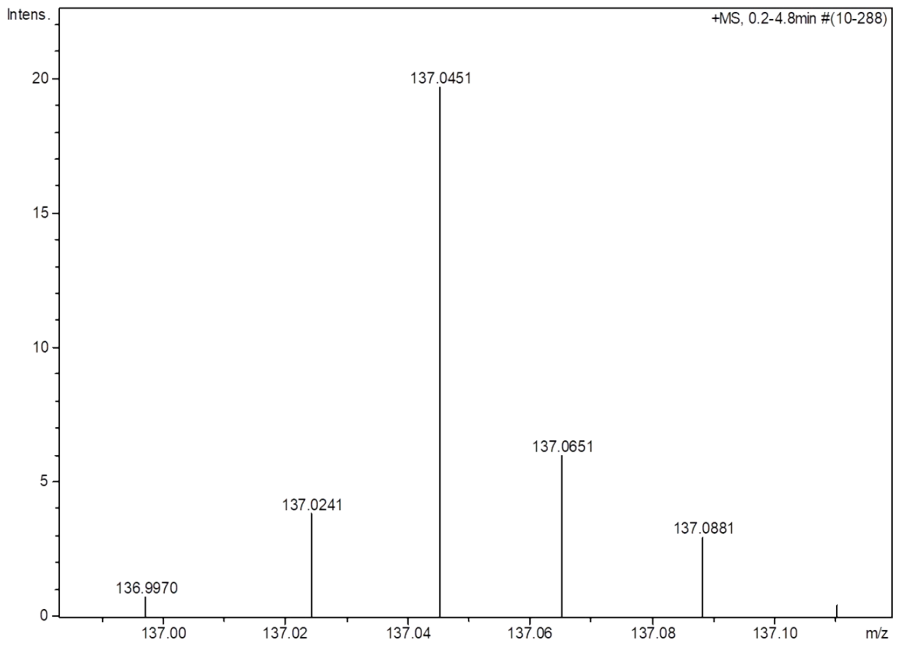

Figure S50. HR-MS (ESI) spectrum of 2-NA in the cabbage extract mixture.

References

S1. T. Ogoshi, M. Hashizume, T. A. Yamagishi and Y. Nakamoto, *Chem. Commun.*, 2010, **46**, 3708-3710.

S2. H. Li, D. X. Chen, Y. L. Sun, Y. B. Zheng, L. L. Tan, P. S. Weiss and Y.-W. Yang, *J. Am. Chem. Soc.*, 2013, **135**, 1570-1576.

S3. X. Li, J. Han, X. Wang, Y. Zhang, C. Jia, J. Qin, C. Wang, J.-R. Wu, W. Fang and Y.-W. Yang, *Mater. Chem. Front.*, 2019, **3**, 103-110.

S4. C. Han, Z. Zhang, G. Yu and F. Huang, *Chem. Commun.*, 2012, **48**, 9876-9878.

S5. G. Yu, B. Hua and C. Han, *Org. Lett.*, 2014, **16**, 2486-2489.

S6. M.-X. Wu and Y.-W. Yang, *Polym. Chem.*, 2019, **10**, 2980-2985.

S7. D. Dai, Z. Li, J. Yang, C. Wang, J.-R. Wu, Y. Wang, D. Zhang, and Y.W. Yang, *J. Am. Chem. Soc.*, 2019, **141**, 4756-4763.

S8. X. Wang, X.-Y. Lou, X.-Y. Jin, F. Liang and Y.-W. Yang, *Research*, 2019, **2019**, 1454562.

S9. X. Li, Z. Li, and Y.-W. Yang, *Adv. Mater.*, 2018, **30**, 1800177.

S10. H. Zhang, F. Liang, and Y.-W. Yang, *Chem. Eur. J.*, 2020, **26**, 198-205.

S11. F. Zhang, Y.-Y. Zhao, H. Chen, X.-H. Wang, Q. Chen and P.-G. He, *Chem. Commun.*, 2015, **51**, 6613-6616.

S12. L. Shao, J. Sun, B. Hua and F. Huang, *Chem. Commun.*, 2018, **54**, 4866-4869.

S13. A. B. Meagan, B.-G. Jorge, J. S. Nicholas, T. P. Aidan, and H. Fraser, *J. Am. Chem. Soc.*, 2018, **140**, 3500-3504.

S14. N. S. Meenakshi, D. C. Sharmistha, B. Nilotpal, P. Haridas, C. B. Achikanath, and M. Jyotirmayee, *J. Phys. Chem. B*, 2015, **119**, 3815-3823.